

Ethene Insertion into Vanadium Hydride Intermediates Formed via Vanadium Atom Reaction with Water or Ethene: A Matrix Isolation Infrared Spectroscopic Study

Matthew G. K. Thompson and J. Mark Parnis*

Department of Chemistry, Chemical Sciences Building, Trent University, Peterborough, Ontario, Canada, K9J 7B8, and Department of Chemistry, Chernoff Hall, Queen's University, Kingston, Ontario, Canada, K7L 3N6

Received August 22, 2007

The reaction of V atoms with H₂O and various concentrations of C₂D₄ in argon has been investigated by matrix isolation infrared (IR) spectroscopy. Both C₂D₆ and CD₂H–CD₂H are observed as the major products of a set of parallel processes involving hydrogenation of ethene where the formal source of hydrogen is either C₂D₄ or H₂O. Portions of the IR spectrum of CD₂H–CD₂H isolated in an argon matrix are observed for the first time. For experiments involving low concentrations of C₂D₄, irradiation of the matrix with light of wavelengths >455 nm results in VH₂ formation, with limited observation of ethene hydrogenation. The source of H₂ is believed to be due to photoelimination of molecular hydrogen from HO–V–H species, during matrix deposition, with OV as an additional product. Recombination of OV with available H₂ in the matrix is proposed as the source of OVH₂ under low ethene conditions. No evidence for VD₂ formation is observed under our conditions. At higher C₂D₄ concentrations, VH₂ formation is suppressed, while products of ethene hydrogenation are maximized. A second process competing with H₂ elimination in which HO–V–H reacts with C₂D₄ is proposed. Parallel reaction schemes involving V atom insertion into the O–H bonds of water or the photoinduced insertion of V atoms into the C–D bonds of C₂D₄ are proposed to account for the observed hydrogenation products. In each mechanism, insertion of C₂D₄ into the V–H or V–D bonds of transient intermediates is followed by photoinduced elimination of the associated ethane isotopomer.

1. Introduction

Hydrocarbons represent an important industrial resource, and thus, understanding mechanistic aspects of their associated chemistry is of considerable value. In particular, metal-atom mediated hydrocarbon transformations remain an interesting area of study, given that these species can often lead to further understanding of key catalytic processes which are synthetically useful. In the specific case of alkene transformations, many of these processes involve the coordination of an alkene molecule by a coordinatively unsaturated metal complex, followed by mechanistic steps such as C–H bond activation, insertion into M–H or M–C bonds, or other organometallic reactions.¹ The diversity of competi-

tive reactions associated with such organometallic species is quite interesting, and understanding the reactivity of coordinatively unsaturated metal complexes is thus of great importance. In particular, early transition metal complexes are of interest, given their significance industrially. Early transition metal complexes are responsible for many major processes such as Ziegler–Natta polymerization,¹ and thus insights into the reaction chemistry of related transition metal-containing intermediates can be particularly valuable. A great deal of information concerning the reactivity and conversions of such species in solution is known. Comparatively less is known for these species reacting under gas-phase conditions. Of those studies in the gas-phase, some provide evidence only for the kinetic reactivity of a metallic species with particular reagents, while evidence of the particular transient

* To whom correspondence should be addressed. E-mail: mparnis@trentu.ca. Phone: +1 705 748 1011, ext. 7297. Fax: +1 705 748 1625.

(1) (a) See for example: Crabtree, R. *The Organometallic Chemistry of the Transition Metals*, 4th ed.; John Wiley & Sons, Inc.: Hoboken, NJ, 2005. (b) Cotton, F. A., Wilkinson, G. *Advanced Inorganic Chemistry*, 5th ed.; Wiley: New York, 1988. (c) Gates, B. C. *Catalytic Chemistry*; John Wiley & Sons, Inc.: Hoboken, NJ, 1992.

(2) Parnis, J. M.; Escobar-Cabrera, E.; Thompson, M. G. K.; Jacula, J. P.; Laffleur, R. D.; Guevara-Garcia, A.; Martinez, A.; Rayner, D. M. *J. Phys. Chem. A* **2005**, *109*, 7046.

(3) Ritter, D.; Carroll, J. J.; Weisshaar, J. C. *J. Phys. Chem.* **1992**, *96*, 10636.

species involved is often unavailable.^{2,3} As a result, the technique of matrix-isolation represents an important bridge for studying the reaction chemistry of metal containing species. This particular work represents an infrared (IR) spectroscopic investigation of the products of atomic vanadium following insertion into simple O–H and C–H containing species, such as water and ethene, under matrix-isolation conditions.

Very recently, Cho and Andrews⁴ have reported the IR spectra of matrix-isolated products of Group V transition metal atoms, generated by laser ablation, reacting with ethene. Their results demonstrate that V atom insertion into the C–H bond of ethene requires excitation of the V atom, consistent with the kinetics results of Ritter and co-workers,³ when studying gas-phase V atom and ethene chemistry. The products of Cho and Andrews show clear evidence for C–H bond insertion products. In particular, species such as the vinyl vanadium hydride, $\text{H}_2\text{C}=\text{CH}-\text{V}-\text{H}$, and a coordinated acetylene dihydride, $(\eta^2-\text{C}_2\text{H}_2)\text{VH}_2$, are formed following irradiation of their matrices with wavelengths corresponding to excitations of matrix-isolated V atoms.⁵ Our recent findings are in agreement with the results of Cho and Andrews, and we present evidence consistent with the reactivity of the transient species identified in their spectra.

Previously, we have observed reactivity for early transition metal atoms with ethene, in which an observed hydrogenation process implicated a reaction of more than one ethene molecule.⁶ The reactions of ethene under high concentration with excited Ti, V, or Nb atoms resulted in the formation of ethane and methane under matrix-isolation conditions. The proposed schemes for rationalizing the ethane formation involve the excited-state atom undergoing multiple insertions into the C–H bond of ethene, a π -coordination of a second C_2H_4 unit, insertion into available M–H bonds, and finally an elimination of the product, ethane.

These results, observed under conditions where the concentration of ethene was very high, were expected to decrease dramatically as the concentration of ethene was diminished; however, subsequent to the publication of this work, we have observed the surprising persistence of ethane formation, even under conditions where only a single ethene might be expected to react. This has led us to consider the availability of other sources of metal hydrides, which provide the key M–H bonds necessary for ethene hydrogenation products to be observed. In the case of low ethene concentration, the only other source of H atoms in our experiments is water, an unavoidable experimental impurity which was previously believed to be uninvolved in the formation of ethane at high ethene concentrations. In light of these new results, we have undertaken an investigation of alkene hydrogenation involving the metal hydride bonds formed by metal atom reactions with either ethene or with water. To differentiate the chemistry of the two potential metal hydride sources, selective experiments involving only C_2D_4 and H_2O have been used as a means of mapping the source of H/D

involved in the overall hydrogenation. This method has proven successful in identifying products implicating both insertion of metal atoms in the C–H (C–D) bond of ethene and the O–H bond of water, as discussed in detail below. In all cases, the insertion of ethene into M–H bonds of the intermediates formed following C–H or O–H bond insertion is believed to be a key step leading to the resultant hydrogenated ethene products.

2. Experimental Details

Specific details of the apparatus used in these experiments have been described elsewhere.⁶ Gas samples are prepared using standard manometric techniques using 0.1–1% (mole ratio) H_2O , purified by freeze–pump–thaw cycles, and 0.1–1% C_2H_4 (99.5%, Aldrich), C_2D_4 (99% atom D, C/D/N Isotopes) or C_2D_6 (99% atom D, C/D/N isotopes) and $\text{CD}_2\text{H}-\text{CD}_2\text{H}$ (99% atom D, Icon Isotopes). Both C_2D_6 and $\text{CD}_2\text{H}-\text{CD}_2\text{H}$ are used for spectroscopic reference. All gas samples are prepared by diluting the reagent gases in high-purity argon (UHP grade, 99.995%, Praxair). Vanadium atoms are generated by resistively heating a thin strip of the pure metal (0.25 mm thickness, 99.5% metal basis, Alfa Aesar) placed between water-cooled copper electrodes using a 30 A alternating current variable power supply, under high vacuum conditions (10^{-7} – 10^{-8} Torr). The rate of deposition of metal atoms is monitored by use of a quartz crystal microbalance to ensure maximum yield of metal atomic species and minimized metal aggregates. Typical metal introduction rates are between 0.3 and 0.5 μmol per hour. Metal atoms are mixed in a flow of the argon (up to ~ 10 mmol per hour) which contains water and/or isotopomers of ethene using an MKS 1100 series mass flow controller. The argon/ethene mixture containing the metal atoms is condensed on a cold CsI spectroscopic window maintained near 17 K using an APD Cryogenics (model HC-2) closed cycle helium refrigeration unit. Irradiation of deposited matrices with light is performed using a Kratos LH150 150W Xe arc lamp and various band-pass filters, where indicated. Typical matrix deposition times are 1 h, unless otherwise specified. In all cases, IR absorption spectra of the condensed matrices are collected using a 1 cm^{-1} resolution Bomem MB 102 spectrometer in absorption mode.

3. Results

Experimental Results. Co-deposition of V atoms in Ar matrices containing C_2H_4 and H_2O under relatively low concentrations of each species (1:2:1000, $\text{H}_2\text{O}/\text{C}_2\text{H}_4/\text{Ar}$) resulted in the observation of C_2H_6 as the major product in the IR spectrum. A set of similar reactions in which the only variable parameter was the flow rate of the gas mixture over a fixed time interval showed a trend of increasing ethane formation following matrix deposition as the flow rate of the gas was increased. Figure 1 demonstrates the variation in the measured peak area (normalized with respect to the highest yield conditions) for three of the major absorption bands of ethane generated by the reaction of V atoms and C_2H_4 in Ar as a function of the gas-flow rate during matrix deposition. At higher flow rates, the yield of ethane was maximized, indicating that such conditions are optimal for exploring the formation of ethane in our apparatus. In all further results, the gas-flow rate used for matrix preparation was 5.00 sccm (standard cm^3 per minute).

(4) Cho, H. G.; Andrews, L. *J. Phys. Chem. A* **2007**, *111*, 5201.

(5) Devore, T. C. *J. Chem. Phys.* **1975**, *62*, 520.

(6) Thompson, M. G. K.; Parnis, J. M. *J. Phys. Chem. A* **2005**, *109*, 9465.

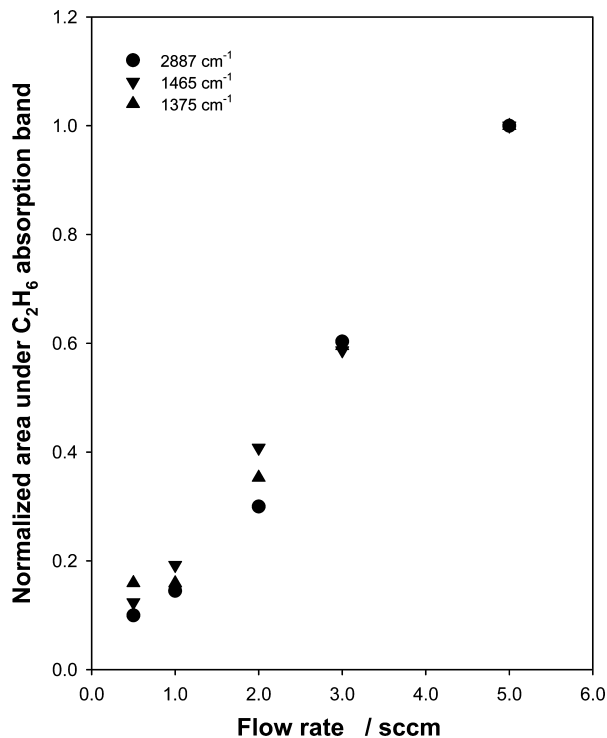


Figure 1. Comparison of ethane yield with gas-flow rate for V + C₂H₄ reaction under matrix isolation conditions.

When V atoms are co-deposited with Ar containing only dilute H₂O, all IR spectral features associated with matrix isolated H₂O are substantially decreased with respect to the spectrum of the same H₂O/Ar mixture without V atoms present. Concurrently, new weak features at 1710 cm⁻¹, 1680 cm⁻¹, and 1029 cm⁻¹ are observed in the spectrum, immediately after deposition. These features correspond to OVH₂, which has been previously isolated in an argon matrix.⁷ Under conditions where the ethene in the matrix is dilute (<1:500 C₂H₄/Ar), these weak features associated with OVH₂ can be increased by annealing the matrix from 17 to 25 K. Surprisingly, no evidence for a feature at 1567 cm⁻¹ is observed, corresponding to the known HO–V–H species,⁷ nor is the feature at 1583 cm⁻¹ observed, originally assigned to HO–V–H by Kauffman et al.⁸ In cases where the concentration of ethene is most dilute (<1:2000 C₂H₄ to Ar), irradiation of V atom-containing matrices with light of wavelengths >455 nm caused the growth of a feature at 1508 cm⁻¹ corresponding to VH₂.⁹ Similar matrices prepared containing 1:2000 C₂D₄/Ar showed continued formation of VH₂ following irradiation, while no evidence for VD₂ was observed. As the only source of H present in these experiments is H₂O, this suggests that a relatively rapid reaction with V and H₂O under deposition conditions occurs, ultimately eliminating molecular hydrogen.

In contrast, as the concentration of C₂D₄ in argon is slowly increased, spectral features corresponding to OVH₂ are

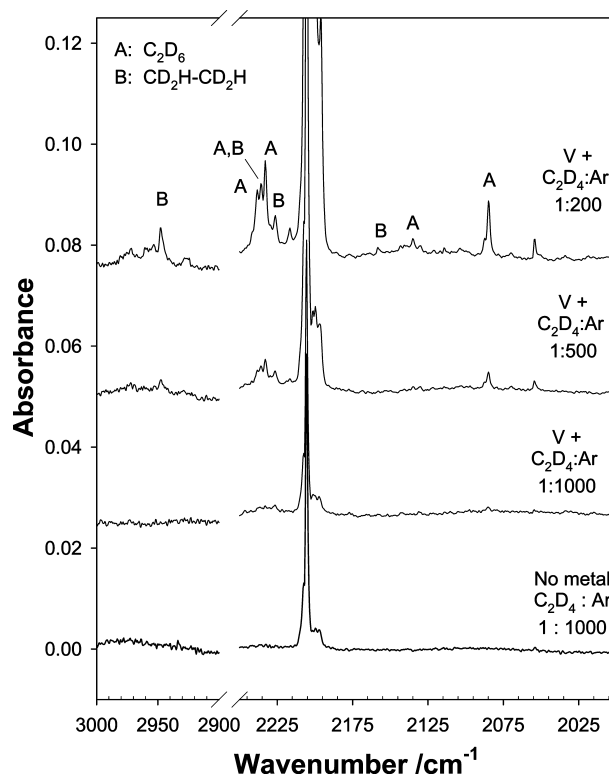


Figure 2. Portions of the IR spectra in the C–H and C–D stretching region for V atoms reacting with H₂O and C₂D₄ isolated in Ar at C₂D₄ concentrations ranging from 0.01% to 0.5% C₂D₄. The bottom reference spectrum containing no metal is of the lowest C₂D₄/Ar concentration. Major product bands have been labeled for clarity, while any unmarked features correspond to C₂D₄ in Ar.

diminished. As the concentration is increased through to 1:200 C₂D₄/Ar, irradiation of the matrix with wavelengths >455 nm no longer shows evidence for VH₂ formation. Instead, a set of strong new features is present on deposition at 2947, 2238, 2235, 2232, 2226, 2216, 2158, 2134, 2084, 1308, 1306, 1302, 1064, and 1057 cm⁻¹ with corresponding increases in intensity as the concentration of C₂D₄ is raised. Additional new features in the region 700–500 cm⁻¹ may be present but are difficult to resolve because of overlapping features of precursor C₂D₄ in this region. Representative spectra demonstrating the increase in these features in the C–D stretching region for V atoms reacting with increasing concentration of C₂D₄ can be seen in Figure 2. A summary of the new features is given as Table 1.

Of these new features, there are two clear sets based on correlation in variation of integrated peak areas as the experimental conditions are changed. One set “A”, at 2238, 2235, 2232, 2216, 2134, and 2084 cm⁻¹ behaved similarly in all experiments in which they are present and occur at wavenumber positions corresponding to the most intense features in the Ar matrix-isolated spectrum of C₂D₆. Thus, the features corresponding to set A are identified as C₂D₆ isolated in Ar. The remaining features, set “B”, at 2947, 2232 (overlapped with C₂D₆), 2226, and 2158, 1308, 1306, 1302, 1064, and 1057 cm⁻¹ shows a similar behavior in all experiments and have the same characteristics of a completely saturated hydrocarbon containing at least one C–H

(7) Zhou, M.; Dong, J.; Zhang, L.; Qin, Q. *J. Am. Chem. Soc.* **2001**, *123*, 135.

(8) Kauffman, J. W.; Hauge, R. H.; Margrave, J. L. *J. Phys. Chem.* **1985**, *89*, 3547.

(9) Xiao, Z. L.; Hauge, R. H.; Margrave, J. L. *J. Phys. Chem.* **1991**, *95*, 2696.

Table 1. Comparison of the IR Absorption Wavenumbers for V Atoms Reacting with H₂O and C₂D₄ in Ar with Corresponding Values for Ethane Isotopomers (C₂D₆ and CD₂H–CD₂H) Directly Isolated in Ar

label	V + H ₂ O + C ₂ D ₄ in Ar	C ₂ D ₆ in Ar	CD ₂ H–CD ₂ H in Ar	C ₂ D ₆ (gas phase) ^a	C ₂ H–CD ₂ H–CD ₂ H (gas phase) ^a	C ₂ –CD ₂ H–CD ₂ H (gas phase) ^a
			2968			
			2965			
			2961			
	2956					2958
			2953			
B	2948		2948		2948	2954
			2929			
A	2238	2238				
A, B	2235	2236	2236			
B		2233	2233			
A, B	2232	2232				
				2229		2229
B	2226		2225	2225		
			2220			
A	2216	2216	2217			
						2196
			2190			
					2182	
			2177			
B	2158		2158			2157
			2154			
						2146
			2143			
A	2134	2134			2136	
			2131			
				2100		
A	2084	2084				
						1340
						1321
B	1308		1308		1309	
B	1306		1306			
B	1302		1302			
						1282
				1158		
						1133
					1120	
						1109
					1107	
				1082		
				1072		
B	1064		1064			1070
						1060
B	1057		1057			
				1055		
						1008
				970		
						900
				852		
					720	
						651
					635	
						618
				594		

^a Data taken from ref 10.

bond but primarily C–D bonds. No other major modes are present in the spectra in which set A and B appeared. As can be seen in Figure 2, the set of features labeled “B” began to appear first in the most dilute spectra containing C₂D₄. As C₂D₄ concentration was increased, the B set of features slowly grew, with a more marked increase in features associated with set A demonstrating that these two species are generated by competitive mechanisms.

Given that the major features observed in set B are observed with concomitant loss of H₂O and C₂D₄ and that the set contained C–H stretching mode absorptions and several C–D stretching mode absorptions similar to those

associated with C₂D₆, we have assigned the features to a saturated hydrocarbon product of V + H₂O + C₂D₄. The simplest saturated hydrocarbon product involving H₂O and C₂D₄, which contains only C–H and C–D bonds, is expected to be an ethane isotopomer of the stoichiometry C₂D₄H₂. Given this stoichiometry, two major isomers are possible: CD₂H–CD₂H (which has two rotational conformations) and CDH₂–CD₃, the latter isomer only anticipated if C–D scrambling is to occur during the reaction. The gas-phase spectrum of CD₂H–CD₂H is known by the work of Van

(10) Van Riet, R. *Ann. Soc. Sci. Bruxelles* **1957**, 71, 102.

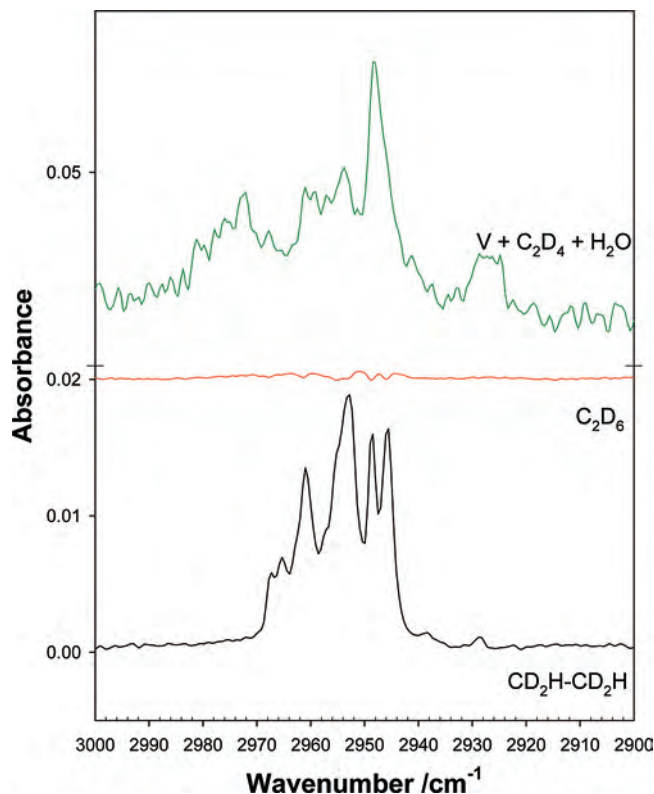


Figure 3. Comparison of the C–H stretching region of the IR spectra of (bottom to top): 1% $\text{CD}_2\text{H}-\text{CD}_2\text{H}$ in Ar, 1% C_2D_6 in Ar, and V atoms co-condensed with Ar containing 0.5% C_2D_4 and 0.01% H_2O . Spectra have been offset by a constant in the vertical axis for clarity. A break in the vertical axis between 0.02 and 0.045 has been made for clarity in comparing this region of the spectrum.

Riet,¹⁰ although the $\text{CH}_2\text{D}-\text{CD}_3$ spectrum is not studied in that work. All of the modes observed in set B are similar to the gas-phase $\text{CD}_2\text{H}-\text{CD}_2\text{H}$ spectrum (see Table 1), although no intensity data for any isotopomers is provided. Thus, the absence of key modes of significant intensity cannot be immediately considered.

To confirm the identify of this species, we have prepared a reference matrix containing $\text{CD}_2\text{H}-\text{CD}_2\text{H}$ in Ar. In Figures 3 and 4, portions of the IR spectra obtained by the co-deposition of V atoms with C_2D_4 and H_2O in Ar is compared with IR spectra of similarly prepared matrices containing only C_2D_6 in Ar or $\text{CD}_2\text{H}-\text{CD}_2\text{H}$ in Ar. As the C_2D_6 and $\text{CD}_2\text{H}-\text{CD}_2\text{H}$ spectra have overlapping bands in some areas, a synthetic spectrum of these two has been prepared by the addition of both spectral traces, for comparison in Figure 4 with the metal containing spectra. In this spectral addition, a factor of 0.5 has been applied to the $\text{CD}_2\text{H}-\text{CD}_2\text{H}$ spectrum in attempt to roughly match the intensity profile to the spectrum obtained where these two species are generated as reaction products. Therefore, such a factor indirectly represents a relative yield of the associated hydrocarbons in the metal containing spectrum.

In Figure 3, the C–H stretching region of the IR spectrum of $\text{CD}_2\text{H}-\text{CD}_2\text{H}$ isolated in Ar is presented. Major features are present in this region at 2968, 2965, 2961, 2953, 2949, 2948, and 2929 cm^{-1} . These values are summarized in Table 1. These features correspond to C–H stretching motion of the $\text{CD}_2\text{H}-\text{CD}_2\text{H}$ molecule, which can exist as two stable

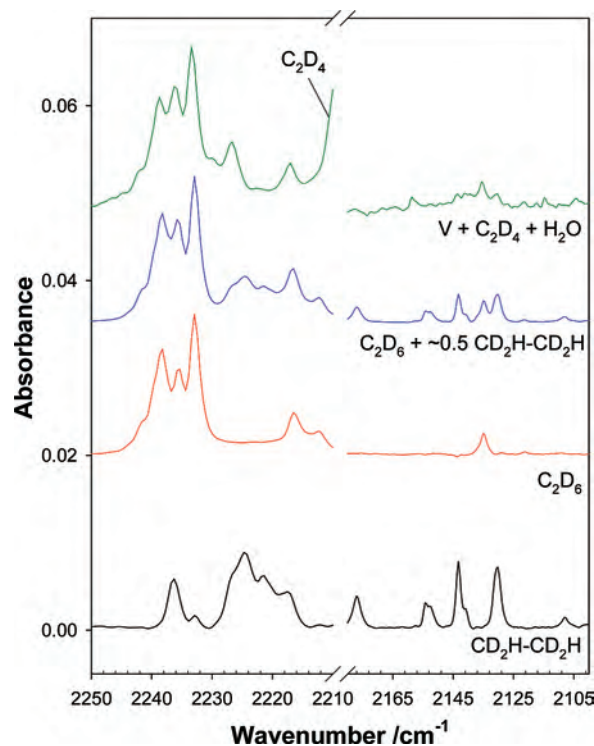


Figure 4. Comparison of the C–D stretching region of the IR spectra of (bottom to top): 1% $\text{CD}_2\text{H}-\text{CD}_2\text{H}$ in Ar, 1% C_2D_6 in Ar, the addition of the bottom two spectra (with the $\text{CD}_2\text{H}-\text{CD}_2\text{H}$ spectrum scaled by 0.5), and V atoms co-condensed with Ar containing 0.5% C_2D_4 and 0.01% H_2O . Spectra have been offset by a constant in the vertical axis for clarity.

rotational conformations. As is expected, C_2D_6 has no absorptions in this region while the IR spectrum of $\text{V} + \text{C}_2\text{D}_4 + \text{H}_2\text{O}$ has its major feature at 2948 cm^{-1} in this region, with other minor features at 2961, 2953, and 2929 cm^{-1} . The presence of only selected modes in the V containing spectrum may suggest a selective formation within the matrix of one of the two isolable rotational conformations of the $\text{CD}_2\text{H}-\text{CD}_2\text{H}$ molecule, as is discussed below.

In Figure 4, the C–D stretching region of the IR spectrum of an argon matrix containing 1% $\text{CD}_2\text{H}-\text{CD}_2\text{H}$ is compared with a 1% $\text{C}_2\text{D}_6/\text{Ar}$ spectrum, and the corresponding IR spectrum obtained with V atoms co-deposited with 0.5% C_2D_4 and 0.01% H_2O in Ar. The major new features in the $\text{CD}_2\text{H}-\text{CD}_2\text{H}$ spectrum are present in this region near 2236, 2233, 2226, 2220, 2216, 2190, 2177, 2154, 2143, and 2131 cm^{-1} . Correspondingly, in the spectrum obtained containing C_2D_6 , new features are present in this region at 2238, 2236, 2233, 2216, 2135, and 2084 cm^{-1} . These features, along with the sets of features A and B described above, are summarized in Table 1, for clarity.

4. Discussion

Increased Flow Rates on Matrix Deposition: Impact of Diffusion. In general, as the flow rate of the gas is increased, the rate of deposition onto the surface of the cold window is accordingly increased. Given that the cooling unit used in our experiments has a fixed rate of removal of heat from the cold tip where a matrix is deposited, the thermal transfer to the apparatus accompanying the higher volume of gas implies that the amount of time necessary for the

matrix to completely freeze will be increasing with the increasing flow rate. As a consequence, this suggests that during matrix formation there is both an enhanced mobility via diffusion of isolated reagents, as well as an enhanced contact time of metal atoms and reagents prior to the complete condensation of the matrix. Correspondingly, one might expect that metal–metal interactions become more and more significant under such conditions.

To investigate the formation of metal–metal aggregates, we have performed experiments of V atoms deposited in pure rare gas matrices in which the flow rate was increased up to 5.00 sccm, using UV–vis spectroscopy as the method of detection. Under the same conditions of metal atom generation as used in our IR experiments, we have not observed a significant amount of vanadium dimer¹¹ to be present, and thus it seems reasonable to discount the increased reactivity as metal dimer chemistry on these grounds. Because the total flow normalized formation of ethane increases effectively linearly with flow rate for the fixed concentration of ethene, as demonstrated in Figure 1, the enhanced yield must be related to an increase in the overall reaction time prior to complete matrix condensation. This increase in time would then allow additional reagent molecules to find transient species in the matrix, allowing for an increased number of successful reaction events.

Recently, similar experiments to those presented here have been performed by Cho and Andrews,⁴ in which the reactions of V atoms with similar concentrations of ethene in Ar under conditions of matrix isolation have been studied. Interestingly, their spectra show no evidence for the formation of ethane as a major product upon deposition. Because the sample preparations and reagents are all similar, it seems clear that there can be only reasons of experimental design that are possible for explaining the divergence in the chemistry. There are three primary differences which may account for this difference in observed chemistry. First, the flow rate used under our conditions is considerably higher than the flow rate of matrix gas introduced in the work of Cho and Andrews (10 mmol per hour compared with 2–4 mmol per hour). Second, the Andrews method uses a laser ablation source for generation of V atoms, while we generate V atoms using thermal vaporization. Our conditions of thermal metal atom vaporization, by comparison, involve the metal filament behaving as a broadband irradiation source. Thus, we may have considerably more resonance excitation of V atoms, or reaction products having an absorption in the visible, during our matrix formation.⁵ Finally, the temperature of the cold tip during matrix deposition conditions of Cho and Andrews is considerably lower (8 K) than that used in our work (17 K). Thus, our matrices will come to complete condensation much more slowly than those of Cho and Andrews, allowing for a greater reaction time in our experiments, during matrix condensation. It is likely that a combination of these factors provides the basis for explaining the differences in our observed chemistry, and that our

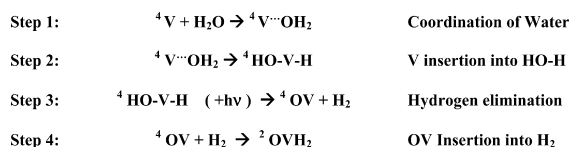
spectra provide evidence for the further reactivity of transient species in the matrix.

Formation Mechanism For OVH₂: Reactivity of HO–V–H in the Absence of C₂D₄. On co-deposition of V atoms in any matrices containing H₂O, a significant depletion of H₂O monomer is always noted when comparing with a matrix in which no metal atoms have been deposited. Additionally, when only H₂O is present (i.e., absence of C₂D₄) in the matrix gas sample, very weak product features are present in the resultant IR spectrum of the matrix containing metal atoms that are consistent with the formation of the known OVH₂ molecule (1710 cm⁻¹, 1680 cm⁻¹, and 1029 cm⁻¹). Annealing of such matrices to 25 K results in the increase of features attributed to OVH₂. In contrast to the results of Zhou et al.,⁷ no evidence for the formation of HO–V–H is observed at 1567 cm⁻¹ in our spectra, nor are features originally assigned at 1583 cm⁻¹ to HO–V–H by Kauffman et al.⁸ observed. Our results confirm that an alternative pathway to OVH₂ formation exists, one that does not involve a direct conversion from HO–V–H by a second O–H bond insertion. Instead, we propose that hydrogen elimination during deposition (possibly photoinduced) from HO–V–H, to form the spin-allowed products OV + H₂, is a major process active in both experimental systems. It is likely that this reaction proceeds spontaneously during condensation, given that the coordination of water and the initial insertion of V into the O–H bond are exothermic by 54.9 kcal mol⁻¹. Since the barrier to elimination of H₂ from HO–V–H is predicted at 35.8 kcal mol⁻¹, this implies that the reaction of V with H₂O to form OV and H₂ is readily accessible provided that the energy of the initial steps is conserved. Once isolated in the matrix, the insertion of the OV into the H–H bond of H₂ would be a second proposed step, resulting in the observed OVH₂ product.

The calculations performed by Zhou et al.⁷ predict that the H₂ addition to OV should be exothermic by approximately 8 kcal mol⁻¹, although a spin crossing is required to convert from the quartet surface of OV to the doublet OVH₂. Given the close relative energies of the reactants and products, it is likely that that only a small barrier to the insertion of OV into the H–H bond exists. In high coordination organometallic systems in which adjacent H ligands are present, elimination of H₂ is often facile.¹ For the lower coordination OVH₂, this might suggest that the only barrier to hydrogen elimination is the endothermicity of the elimination reaction, and hence, the reverse insertion reaction should proceed spontaneously. As such, mild annealing of the matrix could provide the necessary energy for the spontaneous formation of OVH₂ when OV and H₂ are present. If such a mechanism were true, this would represent indirect evidence of OV, which must be present in small concentrations so as not to have a significantly observed IR spectrum under our conditions.

In support of this proposal, we have further investigated the spectra published by Zhou et al.,⁷ and it is clear from their spectra that, even once HO–V–H has been depleted (their Figure 1, spectra c–d), further annealing to 30 K results in increased formation of OVH₂. This increase in OVH₂ is

(11) Ford, T. A.; Huber, H.; Klotzbuecher, W.; Kuendig, E. P.; Moskovits, M.; Ozin, G. A. *J. Chem. Phys.* **1977**, *66* (2), 524.

Scheme 1. Reaction Scheme for the Formation of OVH₂ Following Vanadium Atom Reactions with H₂O

correlated with the loss of matrix isolated OV. No further evidence for HO–V–H formation is observed in their spectra following the 30 K anneal. Our observation of free V atom reaction with liberated molecular H₂ following excitation of V atoms with wavelengths >455 nm to form VH₂ suggests that there is significant availability of H₂, resulting from reactivity of V with water. It seems likely, given the much higher intensity of OV in the spectra of Zhou et al., that their matrices contained similar relative yields of H₂. Thus, Scheme 1 is proposed to account for the observed products in both experimental systems.

Our results are consistent with the steps proposed here, and these steps provide the basis for explaining the formation of ethane isotopomers when ethene is present.

Identification of Ar Isolated CD₂H–CD₂H. It seems clear based on the results section that the series of product features associated with set B in Figures 2–4 is due to the CD₂H–CD₂H isotopomer of ethane isolated in Ar. This species represents a key isotopomer for understanding mechanistic aspects of catalytic hydrogenation studies involving transition metal hydrides, and thus the proper identification of this species is very important. The presence of the key absorptions associated with set B very close to the gas-phase wavenumber values observed by van Riet for CD₂H–CD₂H supports our identification in the matrix. However, the lack of intensity data in van Riet's work, combined with our observation of only a few of the modes of the CD₂H–CD₂H spectrum, leaves some doubt.

In Figures 3 and 4, the C–H and C–D stretching regions of the IR spectrum of CD₂H–CD₂H isolated in Ar are compared with portions of the corresponding IR spectrum obtained following co-deposition of V atoms with C₂D₄ and H₂O in Ar and with the IR spectrum of C₂D₆ in Ar. As can be seen from the collection of data in Table 1, the set of absorptions corresponding to set A in Figure 2 matches very well the spectrum of C₂D₆ isolated in Ar. Similarly, the set of features associated with group B matches very well the spectrum of CD₂H–CD₂H isolated in Ar. However, in the case of the group B features, there are small discrepancies between the CD₂H–CD₂H generated via V/C₂D₄/H₂O reaction and the spectrum acquired from the commercially available CD₂H–CD₂H.

At first this result seems puzzling because selective attrition of spectroscopic features should not be possible. However, the spectrum of CD₂H–CD₂H obtained by deposition of the commercial CD₂H–CD₂H in Ar is obtained by rapidly condensing a gas sample from ambient (298 K) conditions, while the CD₂H–CD₂H generated via V/H₂O/C₂D₄ reaction is synthesized under matrix isolation conditions (approaching 17 K). Given that the CD₂H–CD₂H has two rotational conformers, the matrix condensed with the ambient temper-

ature CD₂H–CD₂H should freeze rapidly enough to preserve the ambient distribution of these conformers when the gas-sample is directly deposited. However, for the CD₂H–CD₂H formed via V + H₂O + C₂D₄, it is likely that (a) the molecule is formed during matrix condensation where $T \ll 298$ K, and that (b) the extrusion of the alkane from the metal intermediate is geometry specific, leading to a preferred conformation of CD₂H–CD₂H when formed in the matrix environment. This selective formation of one conformer over the other would then account for differences in relative intensity that are observed in the two CD₂H–CD₂H spectra and the slight wavenumber differences that are observed in some cases. Furthermore, the CD₂H–CD₂H synthesized when V atoms are present is isolated in a matrix containing C₂D₄. Therefore, the presence of the C₂D₄ in the Ar lattice may disrupt slightly the environment of the isolated CD₂H–CD₂H molecules, leading to slight shifts in the corresponding observed wavenumber values. Finally, the presence of related isotopomeric impurities in the commercial CD₂H–CD₂H sample may give rise to additional spectroscopic signatures that would not be present in the V/C₂D₄/H₂O spectrum. Therefore, on the basis of the number of matching modes and the close wavenumber and intensity values in all cases, we assign the set B features to CD₂H–CD₂H.

Formation Mechanism For CD₂H–CD₂H: Reactivity of HO–V–H in the Presence Of C₂D₄. As the relative amount of C₂D₄ in the matrix gas sample is increased, evidence for metal–water reaction products produced in the later steps of Scheme 1 decreases rapidly. This suggests that a competitive pathway to the formation of OVH₂ exists, when C₂D₄ is present. Such an observation implies either that (a) once formed, the OVH₂ species is consequently reacting with C₂D₄, or (b) a precursor to the formation of OVH₂ is reacting with C₂D₄, inhibiting OVH₂ formation. Because the concentration of C₂D₄ is increased in our experiments, the number of collisions of any species isolated in the matrix with C₂D₄ is consequently increasing. Given that evidence for the formation of VH₂ shuts down as C₂D₄ increases, this implies that the rate of H₂ elimination from HO–V–H is being decreased by some competitive step. Correspondingly, when neither the VH₂ or OVH₂ species are observed in the spectra, there is a product with a new C–H bond formed (CD₂H–CD₂H), and thus it seems evident that the precursor HO–V–H species is being consumed prior to elimination of H₂. The most likely competitive reaction step would involve a π -coordination of a C₂D₄ molecule into one of the vacant sites of the HO–V–H species. Unlike the repulsive electron configuration of the neutral V atom, the oxidized HO–V–H species should have the capacity to coordinate such a π donating ligand easily, forming an HO–VH(η^2 -C₂D₄) isomer.

To generate the final CD₂H–CD₂H product, the formation of the C–H bond must occur. As the HO–VH(η^2 -C₂D₄) isomer has the requisite V–H and C₂D₄ unit, an insertion of C₂D₄ into the V–H bond seems likely. This would suggest the formation of an HO–V–CD₂–CD₂H species, under our reaction conditions. This species is analogous to the

Scheme 2. Proposed Reaction Steps for the Hydrogenation Of C₂D₄ Following Reaction of Atomic V with Water

Step 1:	$V + H_2O \rightarrow V^{\cdots}OH_2$	H ₂ O coordination
Step 2:	$V^{\cdots}OH_2 \rightarrow HO-V-H$	O-H insertion by V
Step 3:	$HO-V-H + C_2D_4 \rightarrow HO-VH(\eta^2-C_2D_4)$	C ₂ D ₄ π-coordination
Step 4:	$HO-VH(\eta^2-C_2D_4) \rightarrow HO-V-CD_2CD_2H$	C ₂ D ₄ insertion in V-H
Step 5:	$HO-V-CD_2CD_2H + hv \rightarrow OV + CD_2H-CD_2H$	CD ₂ H-CD ₂ H elimination
Net:	$V + H_2O + C_2D_4 + hv \rightarrow OV + CD_2H-CD_2H$	Overall

Scheme 3. Proposed Reaction Steps for the Sacrificial Hydrogenation of C₂D₄ Following Reaction of Photoexcited V with 2 C₂D₄

Step 1:	$V + hv \rightarrow V^*$	photoexcitation of V
Step 2:	$V^* + CD_2=CD_2 \rightarrow D_2C=DC-V-D$	C-D insertion by V
Step 3:	$D_2C=DC-V-D + C_2D_4 \rightarrow D_2C=DC-VD(\eta^2-C_2D_4)$	C ₂ D ₄ π-coordination
Step 4:	$D_2C=DC-VD(\eta^2-C_2D_4) \rightarrow D_2C=DC-V-CD_2-CD_3$	C ₂ D ₄ insertion in V-D
Step 5:	$D_2C=DC-V-CD_2-CD_3 + hv \rightarrow (\eta^2-C_2D_2)V + CD_3-CD_3$	C ₂ D ₆ elimination
Net:	$V + 2 C_2D_4 + hv \rightarrow (\eta^2-C_2D_2)V + C_2D_6$	Overall

HO–V–H species, with the V–H bond replaced with a V–CD₂CD₂H group. Elimination of the alkyl group with the H from the HO– moiety would lead to the formation of OV and CD₂H–CD₂H as products. This step is completely analogous to the case of HO–V–H, although one would expect the elimination of an alkane product from HO–V–CD₂CD₂H to be less favorable than the H₂ elimination because of the directionality of the orbital associated with the metal alkyl bond. As such, the barrier to this elimination may be quite large, and this step may require photoexcitation to eliminate the alkane product. Given that the features associated with CD₂H–CD₂H in our experiments behave as one would expect for this proposed chemistry, we suspect that these steps are involved in the major mechanism governing the formation of CD₂H–CD₂H in our matrix experiments. This chemistry is summarized as Scheme 2. In this mechanism, the later steps generate OV as a major product. This product is not observed in our IR spectra when C₂D₄ is present, and we propose that it is possible that the OV species may continue to be active as a hydrogenation catalyst, involving additional water or ethene molecules, following a scheme similar to Scheme 2 or Scheme 3.

Formation Mechanism for CD₃-CD₃: Reactivity of d³-Vinyl-V–D in the Presence of C₂D₄. Given that water is significantly depleted in our experiments when V atoms are present, we first considered the formation of C₂D₆ solely in terms of OV chemistry. At lower concentration of C₂D₄ in Ar, irradiation of our matrices with light >455 nm causes the increase of features at wavenumber values consistent with the C–H/C–D bond insertion intermediates identified by Cho and Andrews for V atoms reacting with ethene.⁴ Similar C–H bond insertion intermediates for which the metal center bears an O atom would be expected to appear at wavenumber positions significantly blue-shifted from the observed insertion intermediates. This statement is based on the calculated vibrational spectrum of a metal atom C–H bond insertion into ethene, in which the metal atom also bears an O, and supports the claims of Cho and Andrews who suggest that the metal hydride stretching frequency shifts to higher energy

as the valency of the V complex increases.⁴ Thus, the likelihood of the sacrificial hydrogenation of ethene involving solely OV is low, but the reactivity of OV cannot be completely eliminated based on the available results.

The presence of significant C₂D₆ with the maximum concentration of C₂D₄ at 0.5% in Ar demonstrates that there is significant availability of C₂D₄ molecules to matrix isolated species during deposition. The only possible formation mechanism of C₂D₆ involves the reaction of at least two C₂D₄ molecules. Given that V atoms must also be excited by a photon prior to direct reaction with C₂D₄, plenty of C₂D₄ must be available near a metal atom under high C₂D₄ concentration deposition conditions to compete with resonant emission. This suggests that, following absorption of a photon, the reaction of excited V atoms with C₂D₄ is quite rapid, and that the rate of collision with C₂D₄ is much greater than the rate of V atom collision with H₂O. Indeed, the onset of C₂D₆ as the major reaction product at higher concentrations of C₂D₄ suggests that the excitation of V and subsequent reaction steps exclusively with C₂D₄ units must be very rapid to compete with CD₂H–CD₂H formation efficiently.

It is anticipated that our observation of C₂D₆ is generated via the reaction of additional C₂D₄ units with the metal C–D insertion intermediates characterized by Cho and Andrews, which are generated in our matrices by light from the filament during deposition. In our previous work involving low concentration of ethene in Ar, features very similar to the bond insertion intermediates identified by Cho and Andrews are observed in our spectra, immediately following deposition.⁴ We thus propose that, when the concentration of C₂D₄ is raised, these insertion species are rapidly consumed in a fashion analogous to HO–V–H (in Scheme 2). The analogous steps following V atom insertion into the C–D bond of C₂D₄ are summarized as Scheme 3.

Following this scheme, the associated vinyl group on the initial C–D insertion intermediate is analogous to the hydroxyl group of the HO–V–H species. The absorption of the V–H stretch in the IR for both the HO–V–H and H₂C=HC–V–H species is quite similar (1567 cm^{–1} and 1573 cm^{–1}), supporting the similar chemical properties of these two ligands. Additionally, in the structure of the vinyl hydride given by the calculations of Cho and Andrews, the geometry of the vinyl group is such that the requisite hydrogen on the CH₂ end is present in a favorable geometry for elimination, as proposed in Step 5 of Scheme 3.

As additional support of all three schemes, spectroscopic evidence consistent with observation of all of the primary transient species, such as HO–V–H and the D₂C=DC–V–D, has been observed. Additionally, in most cases, no spin conversion is required to form products. In the case of the initial transient species formed in Scheme 3, the requirement of photons >420 nm to induce the C–D bond insertion is definitely necessary, and certainly the light emitted by the filament during our metal deposition experiments yields significant intensity in this region. Given that our experiments have demonstrated conclusively that species in the matrix can then be expected to interact with a further C₂D₄ molecule, all of the steps listed in these schemes seem plausible.

The absence of spectroscopic features corresponding to some of the transient species implicated in these schemes is, at first, somewhat perplexing. Considering first that several of the implicated steps involve the formation of OV as a final product, it is interesting to note that, even under the conditions where the largest yields of ethane isotopomers are generated, no significant absorption at 987 cm^{-1} corresponding to matrix-isolated OV is observed.⁷ However, under most conditions, a significant amount of C_2D_6 is observed, which requires that a larger fraction of the V atoms are reacting selectively with C_2D_4 and not with water. As a result, the total number of V atoms reaching the matrix must be distributed between OV and $(\eta^2\text{-C}_2\text{D}_2)\text{V}$ species (or their further reaction products). We propose that the lack of observation of these key species in our spectra is due to the small concentrations limited by the number of V atoms. As a result, while these species must be formed, their weak absorption spectra inhibit their direct observation, or their continued reactivity limits their accumulation in the matrix environment.

The absence of newly proposed intermediates such as $\text{HO-VH}(\eta^2\text{-C}_2\text{D}_4)$, $\text{HO-V}(-\text{CD}_2\text{CD}_2\text{H})$, $\text{D}_2\text{C}=\text{CD-V}(\eta^2\text{-C}_2\text{D}_4)$, or $\text{D}_2\text{C}=\text{CD-V-CD}_2\text{-CD}_3$ can be explained using thermodynamic arguments. Thermochemical calculations involving second-row transition metal atom hydrides reacting with ethene are expected to have only a small barrier to, or even a barrierless, insertion of ethene into the M-H bonds of L_nMH_x species.¹² This argument, or a similar one, for first row transition metal species with increasing numbers of coordinated ligands may still hold true. If the insertion of C_2D_4 into the V-H bond of $\text{HO-V-H}(\eta^2\text{-C}_2\text{D}_4)$ were barrierless, $\text{HO-V-CD}_2\text{-CD}_2\text{H}$ would be formed rapidly, and thus the precursor would not be observed. Once formed in the matrix, $\text{HO-V-CD}_2\text{-CD}_2\text{H}$ would be subject to prolonged irradiation by the filament and thus may be expected to photoeliminate the $\text{CD}_2\text{H-CD}_2\text{H}$ product.

In each of the schemes presented above, the π -coordination of the ethene molecule which formally ends up as the ethane product occurs at the monohydride intermediate. Given that key species implicated in these schemes are not directly observed, we cannot immediately eliminate a mechanism by which the π -coordination occurs following a second insertion of V into additional O-H or C-D bonds of the HO- or $\text{D}_2\text{C}=\text{DC-}$ coordinated ligands. However, given that both of the dihydrido- products require spin conversion, it is very likely that the formation of these species is slow by direct O-H or C-D insertion because of a kinetic impediment. Thus, it seems more likely to coordinate the alkene to the monohydride intermediates in all cases, for which all of the following steps in the schemes proceed via spin conserved surfaces, rather than invoking steps in which spin interconversion must first occur.

(12) Siegbahn, P. E. M. *J. Am. Chem. Soc.* **1993**, *115*, 5803.

Absence of V + H₂O + C₂D₄ Chemistry in Earlier Work. Under conditions where ethane was originally observed, we noted a significant loss of ethene dimer¹³ and the ethene/water 2:1 hydrogen bonded complex.¹⁴ Similar experiments with C_2D_4 in high concentration showed the formation of C_2D_6 and CD_4 only, while losses of the ethene dimer and ethene/water 2:1 complex were still observed. As a result, we concluded that ethane formation involving H_2O as the formal source of hydrogen was not directly involved in the overall hydrogenation process.⁶ Clearly, the formation of $\text{CD}_2\text{H-CD}_2\text{H}$ under these new reaction conditions implicates parallel reactivity involving H_2O , which ultimately leads to ethane formation. Thus some explanation for the lack of H_2O observed reactivity in the earlier work is required.

The simplest explanation seems to lie in the impact of concentration of ethene, for which the earlier results employed a concentration of ethene that was approximately 10–20 fold increased, compared from our most concentrated experiments in this work. Noting that a mere 2-fold increase in the concentration of C_2D_4 in this work results in significant increase in the C_2D_6 product, then it is not unreasonable to expect that the same process at 10–20 times the C_2D_4 concentration would ultimately dominate, outcompeting every other mechanism. If such a supposition were true, then the formation of reaction products involving V + H_2O chemistry may not be significantly observed, compared from the overwhelming C_2D_4 chemistry. Thus, while the chemistry may have been present, the product yields may simply have been too small to observe, in deference to the formation of C_2D_6 .

5. Summary and Conclusions

Vanadium hydrides formed by the insertion of the metal atom into the O-H bonds of water or the C-D bonds of C_2D_4 are able to further react with additional deuterated ethene molecules to form isotopomers of ethane as major products. Consequently, the major features of the IR spectrum of $\text{CD}_2\text{H-CD}_2\text{H}$ isolated in an argon matrix have been observed for the first time. A mechanism involving C-H or O-H bond insertion by V atoms, alkene insertion, and subsequent elimination of ethane is proposed. These mechanisms are consistent with the IR data observed in this work.

Acknowledgment. M.G.K.T. acknowledges the support of the NSERC PGS program for scholarship funding. Additional support from the NSERC Discovery grant program is gratefully acknowledged.

IC701653V

- (13) (a) Cowieson, D. R.; Barnes, A. J.; Orville-Thomas, W. J. *J. Raman Spectrosc.* **1981**, *10*, 224. (b) Rytter, E.; Gruen, D. M. *Spectrochim. Acta* **1979**, *35A*, 199.
 (14) Thompson, M. G. K.; Lewars, E. G.; Parnis, J. M. *J. Phys. Chem. A* **2005**, *109*, 9499.